



**HAL**  
open science

## Experimental Determination of Dissociative Recombination Reaction Pathways and Absolute Reaction Cross-Sections of $\text{CH}_2\text{OH}^+$ , $\text{CD}_2\text{OD}^+$ and $\text{CD}_2\text{OD}_2^+$

Mathias Hamberg, Wolf Dietrich Geppert, Richard D Thomas, Vitaly Zhaunerchyk, Fabian Österdahl, Anneli Ehlerding, Magdalena Kaminska, Jacek Semaniak, Magnus af Ugglas, Anders Källberg, et al.

► **To cite this version:**

Mathias Hamberg, Wolf Dietrich Geppert, Richard D Thomas, Vitaly Zhaunerchyk, Fabian Österdahl, et al.. Experimental Determination of Dissociative Recombination Reaction Pathways and Absolute Reaction Cross-Sections of  $\text{CH}_2\text{OH}^+$ ,  $\text{CD}_2\text{OD}^+$  and  $\text{CD}_2\text{OD}_2^+$ . *Molecular Physics*, 2007, 105 (05-07), pp.899-906. 10.1080/00268970701206642 . hal-00513081

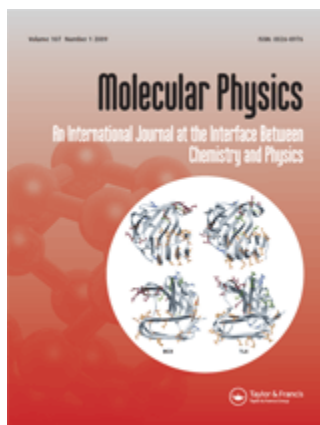
**HAL Id: hal-00513081**

**<https://hal.science/hal-00513081>**

Submitted on 1 Sep 2010

**HAL** is a multi-disciplinary open access archive for the deposit and dissemination of scientific research documents, whether they are published or not. The documents may come from teaching and research institutions in France or abroad, or from public or private research centers.

L'archive ouverte pluridisciplinaire **HAL**, est destinée au dépôt et à la diffusion de documents scientifiques de niveau recherche, publiés ou non, émanant des établissements d'enseignement et de recherche français ou étrangers, des laboratoires publics ou privés.



**Experimental Determination of Dissociative Recombination  
Reaction Pathways and Absolute Reaction Cross-Sections of  
CH<sub>2</sub>OH<sup>+</sup>, CD<sub>2</sub>OD<sup>+</sup> and CD<sub>2</sub>OD<sub>2</sub><sup>+</sup>**

Journal:	<i>Molecular Physics</i>
Manuscript ID:	TMPH-2006-0052.R1
Manuscript Type:	Full Paper
Date Submitted by the Author:	30-Dec-2006
Complete List of Authors:	<p>Hamberg, Mathias; Stockholm University, Physics Department            Geppert, Wolf; Stockholm University, Physics; Stockholm University, Physics            Thomas, Richard; Stockholm University, Physics Department            Zhaunerchyk, Vitaly; Stockholm University, Physics Department            Österdahl, Fabian; Royal Institute of Technology, Physics Department            Ehlerding, Anneli; Stockholm University, Physics Department            Kaminska, Magdalena; Swietokrzyska Akademy            Semaniak, Jacek; Swietokrzyska Akademy            af Ugglas, Magnus; Stockholm University, Physics Department            Källberg, Anders; Stockholm University, Manne Siegbahn Laboratory            Paál, András; Stockholm University, Manne Siegbahn Laboratory            Larsson, Mats; Stockholm University, Physics Department</p>
Keywords:	Dissociative recombination , Ion-electron interaction, CRYRING, comets

1  
2  
3  
4  
5  
6  
7  
8  
9  
10  
11  
12  
13  
14  
15  
16  
17  
18  
19  
20  
21  
22  
23  
24  
25  
26  
27  
28  
29  
30  
31  
32  
33  
34  
35  
36  
37  
38  
39  
40  
41  
42  
43  
44  
45  
46  
47  
48  
49  
50  
51  
52  
53  
54  
55  
56  
57  
58  
59  
60



For Peer Review Only

# Experimental Determination of Dissociative Recombination Reaction Pathways and Absolute Reaction Cross-Sections of $\text{CH}_2\text{OH}^+$ , $\text{CD}_2\text{OD}^+$ and $\text{CD}_2\text{OD}_2^+$

M. HAMBERG<sup>†</sup>, W. D. GEPPERT<sup>\*†</sup>, R. D. THOMAS<sup>†</sup>, V. ZHAUNERCHYK<sup>†</sup>, F. ÖSTERDAHL<sup>†</sup>, A. EHLERDING<sup>†</sup>, M. KAMINSKA<sup>‡</sup>, J. SEMANIAK<sup>‡</sup>, M. AF UGGLAS<sup>†</sup>, A. KÄLLBERG<sup>§</sup>, A. PAAL<sup>§</sup>, [A. SIMONSSON<sup>§</sup>](#) and M. LARSSON<sup>†</sup>

<sup>†</sup> Department of Physics, Stockholm University, Stockholm, Sweden

<sup>‡</sup> Institute of Physics, Świętokrzyska Academy, Kielce, Poland

<sup>§</sup> Manne Siegbahn Laboratory, Stockholm, Sweden

\*Corresponding author. E-mail: wgeppert@hotmail.com

## Abstract

Measurements of the cross-sections and branching ratios of the dissociative recombination of the ions  $\text{CH}_2\text{OH}^+$ ,  $\text{CD}_2\text{OD}^+$  and  $\text{CD}_2\text{OD}_2^+$  have been performed at the CRYRING storage ring located in Stockholm, Sweden. Evaluation of the data yielded reaction rate coefficients of:  $7.0 \times 10^{-7} (T/300)^{-0.78} \text{ cm}^3 \text{ mol}^{-1} \text{ s}^{-1}$  for  $\text{CH}_2\text{OH}^+$ ;  $7.5 \times 10^{-7} (T/300)^{-0.70} \text{ cm}^3 \text{ mol}^{-1} \text{ s}^{-1}$  for  $\text{CD}_2\text{OD}^+$  and  $1.51 \times 10^{-6} (T/300)^{-0.66} \text{ cm}^3 \text{ mol}^{-1} \text{ s}^{-1}$  for  $\text{CD}_2\text{OD}_2^+$ . Calculation of the branching ratios for  $\text{CH}_2\text{OH}^+$  and its deuterated isotopologue gave the following results for the DR reaction channels involving C-O bond fission:  $\text{H}_2\text{O}+\text{CH}$  (2.2%) and  $\text{CH}_2+\text{OH}$  (5.5%) in the reaction of  $\text{CH}_2\text{OH}^+$  as well as  $\text{D}_2\text{O}+\text{CD}$  (5%) and  $\text{CD}_2+\text{OD}$  (18%) for the dissociative recombination of  $\text{CD}_2\text{OD}^+$ . The remainder of the reaction flux kept the C-O bond intact: 92% for  $\text{CH}_2\text{OH}^+$  and 77% for  $\text{CD}_2\text{OD}^+$ , respectively. Other recent measurements on the  $\text{CH}_3\text{OH}_2^+$  ion indicate dominating bond breaking between the heavy atoms, which is conversely to this experiment. For  $\text{CD}_2\text{OD}_2^+$  CO-bond breaking was observed for 57% of the reaction flux.

**Keywords:** Dissociative Recombination, Ion electron interaction, CRYRING, comets

**AMS Subject Classification:** 85-05

## 1 Introduction

Experimental studies of the dissociative recombination (DR) processes of the astrophysically important hydroxymethyl ion ( $\text{CH}_2\text{OH}^+$ ), its deuterated isotopologue ( $\text{CD}_2\text{OD}^+$ ) and methyleneoxonium ion ( $\text{CD}_2\text{OD}_2^+$ ) [1--2] have been performed at the Cryogenic Storage Ring (CRYRING) located at the Manne Siegbahn Laboratory, Stockholm University, Sweden. DR is a fast process in which a free electron recombines with a molecular ion and the formed neutral molecule subsequently disintegrates into smaller fragments. It is one of the dominant reactions occurring in the interstellar medium such as dark interstellar clouds [3--4][8] and comas of comets [1]. It is also an important process in aeronomical plasmas [5], such as

Deleted: ( T

Deleted: those

Deleted: and

Deleted: atoms which

Deleted: Conversely, for the  $\text{CH}_3\text{OH}_2^+$  ion, the pathways preserving the bond between the heavy atoms dominate.

Deleted: comets[

Deleted: reaction

northern lights [6] and lightning [7], as well as in artificial plasmas such as those encountered in fusion reactors and combustion processes [8], almost everywhere where there is a plasma cold enough to contain molecular ions.

Deleted: there

In the coma of comet Halley, investigated by the ion mass spectrometer (IMS) on the Giotto spacecraft, the 31 amu/e peak observed in the ion mass spectra is thought to be dominated by the protonated formaldehyde ion  $\text{CH}_2\text{OH}^+$ , from which one can conclude the  $\text{H}_2\text{CO}$  density [9].  $\text{CH}_2\text{OH}^+$  together with  $\text{CH}_3\text{OH}_2^+$  [10] are amongst the major ions in the inner coma and have therefore been used in obtaining the number density of many important neutral species in the same region [1,10]. In this region,  $\text{CH}_2\text{OH}^+$  ions are thought to be produced by reactions of the following species:  $\text{H}_3\text{O}^+ + \text{H}_2\text{CO}$ ;  $\text{CH}_3^+ + \text{CH}_3\text{OH}$ ;  $\text{CH}_2^+ + \text{H}_2\text{O}$ ;  $\text{H}_2\text{CN}^+ + \text{H}_2\text{CO}$ ;  $\text{H}_2\text{O}^+ + \text{H}_2\text{CO}$ ;  $\text{O}^+ + \text{CH}_3\text{OH}$  and  $\text{CH}_3\text{OH} + \text{h}\nu$  [1].  $\text{CH}_2\text{OH}^+$  is also believed to be produced through depletion of the astrophysically important ion  $\text{HOC}^+$  in the reaction

Deleted: +



and has also been included in model calculations concerning the  $\text{HCO}^+ / \text{HOC}^+$  abundance ratio in dense interstellar clouds [11]. Reactions other than DR, which dominates at radial distances greater than 1000 km, for the degradation of  $\text{CH}_2\text{OH}^+$  in the coma of Halley are assumed to consist of proton transfer reactions to  $\text{H}_2\text{O}$ , which dominates at low radial distances, and to  $\text{NH}_3$ ,  $\text{H}_2\text{S}$ , and  $\text{HCN}$  [1].

One of the minor molecular ions in the coma of Comet Halley that was detected by the IMS on the Giotto spacecraft, might be the methanol ion  $\text{CH}_3\text{OH}^+$ , contributing to the peak with the mass-to-charge ratio of 32 [1]. Its abundance at the radial distance of  $\sim 300$  km represents approximately 0.05 % of all ions emitted/observed around the comet. The main production routes of  $\text{CH}_3\text{OH}^+$  ion in the coma are photon, photoelectron and auroral electron impact ionization of methanol. Proton transfer to  $\text{H}_2\text{O}$  and dissociative recombination are the main pathways of ion destruction. At the distances of 100, 1000 and 5000 km from the comet's core, the relative contribution of the former process to the destruction is thought to be 99.8 %, 94.1 % and 80 %, respectively, where the rest is made up mainly by DR.

DR reactions have been extensively studied over the last three decades using a variety of experimental methods such as the flowing afterglow techniques [12--13] and heavy-ion storage rings [14]. A theory capable of accurately predicting the reaction rate and product distributions for the DR of polyatomic molecular ions has yet to be formulated. The earliest attempts, such as the theory by Bates [15] stating that the channel or the channels involving the least rearrangement of valence bonds should be favoured, are not able to predict the experimental findings on even small polyatomic molecules [16]. This has also been observed for the important interstellar ion such as  $\text{CH}_3\text{OH}_2^+$  [17]. Here the experiments yielded surprising results in which the fraction of the reaction flux channel leading to methanol and a hydrogen atom ( $\text{CH}_3\text{OH} + \text{H}$ ) is around 5%, though it is precisely this channel that involves the least valence bond rearrangements within the molecule and which, according to Bates, should dominate [15]. Experimental observations such as these have a big impact on the results of astronomical model calculations [18], where the experimentally determined values can be used instead of often highly uncertain assumptions.

Deleted: suggested

Deleted: an

Deleted: protonated methanol

Formatted

Formatted

The next step is to investigate structure-related ions in order to pinpoint trends that might occur in the distributions of branching ratios of DR reactions of similar ions, which then can eventually lead to new theoretical models of the DR process. For this reason we have investigated the DR of  $\text{CH}_2\text{OH}^+$ ,  $\text{CD}_2\text{OD}^+$ , and

Deleted: .

CD<sub>2</sub>OD<sub>2</sub><sup>+</sup> ions with electrons at a relative collision energy of 0 eV. The energetically viable pathways are listed in Table 1, with reaction enthalpies calculated from ref [19--20].

Table 1. Open DR reaction channels.

Ion	Fragments	Reaction enthalpies (eV)	Channel		
CD <sub>2</sub> OD <sup>+</sup>	CO <sub>D<sub>x</sub></sub>	yD	zD <sub>2</sub>	α	
	CO	3D		1.5	
	CDO	2D		2.2	
	CO	D <sub>2</sub>	D	6.1	
	CD <sub>2</sub> O	D		6.2	
	CDO	D <sub>2</sub>		6.8	
	CD	D <sub>2</sub> O		3.7	
	CD <sub>2</sub>	OD		2.9	
CH <sub>2</sub> OH <sup>+</sup>	CO <sub>H<sub>x</sub></sub>	yH	zH <sub>2</sub>	α <sub>2</sub>	
	CO	3H		1.7	
	CHO	2H		2.3	
	CO	H <sub>2</sub>	H	6.2	
	CH <sub>2</sub> O	H		6.2	
	CHO	H <sub>2</sub>		6.8	
	CH	H <sub>2</sub> O		3.6	
	CH <sub>2</sub>	OH		2.9	
CD <sub>2</sub> OD <sub>2</sub> <sup>±</sup>	CO <sub>D<sub>x</sub></sub>	yD	zD <sub>2</sub>	α <sub>3</sub>	
	CD <sub>3</sub> O	D		6.3	
	CD <sub>2</sub> O	D <sub>2</sub>		10.0	
	CD <sub>2</sub> O	2D		5.4	
	CDO	D <sub>2</sub>	D	6.0	
	CDO	3D		1.4	
	CO	2D <sub>2</sub>		9.9	
	CO	D <sub>2</sub>	2D	5.3	
	CO	4D		0.7	
	CD <sub>x</sub>	ODy	zD <sub>2</sub>	aD	β <sub>3</sub>
	CD <sub>4</sub>	O		7.0	
	CD <sub>3</sub>	OD		6.9	
	CD <sub>3</sub>	O	D	2.4	
	CD <sub>2</sub>	D <sub>2</sub> O		7.3	
	CD <sub>2</sub>	OD	D	2.1	
	CD <sub>2</sub>	O	D <sub>2</sub>	2.2	
	CD	D <sub>2</sub> O	D	2.9	
	CD	OD	D <sub>2</sub>	2.2	
	C	D <sub>2</sub> O	D <sub>2</sub>	3.9	

In the table the letters x are used for denoting the number of hydrogen/deuterium atoms. y, z and a are used for visualization of the possible pathways. Reaction enthalpies were calculated from ref. [19--20]. Values for deuterated species are applied if found in the references.

Deleted: . F

Deleted: for the reaction

Deleted: of these ions

Deleted: ,

Deleted: t

Deleted: energy release

Deleted: Energy Release

Formatted

Formatted

Formatted

Formatted

Formatted

Formatted

Formatted

Formatted

Formatted

Deleted: ¶

Table 1. Open DR reaction channels [1]

Deleted: Energy release values

## 2 Experiment

The experiment took place at the heavy ion storage ring CRYRING, Stockholm, Sweden. The ring consists of twelve straight sections with bending magnets in between giving a total circumference of 51.6 m. The experimental procedure has previously been described in detail elsewhere [21] and is therefore only briefly described here.

### 2.1 Ion production, injection and acceleration

The ions were produced in a hollow cathode ion source by discharge ionization in a mixture of either methanol/H<sub>2</sub> or deuterated methanol/D<sub>2</sub>. By pulsing the injection process, during typically a few tens of milliseconds, sample consumption and sooting as well as the base pressure in the ion source can be kept at a very low level (typically  $\sim 10^{-6}$  Torr) [22]. This approach also helps to improve the time profile of the discharge due to synchronization of the discharge with the gas pulse. The ions produced (mass 31, 34 and 36 amu respectively) were then accelerated by 40 kV and mass selected by a dipole magnet. However, several isomers of the probe ions might be formed in the ion source. No selection of specific isomers is possible under the current set-up and no investigation into the presence of different isomers has been undertaken for the three species in this experiment but for reasons explained in the Discussion section it is justified to assume that the ion beam consists of the specific isomers given here. In order to avoid contamination of the ultra high vacuum of  $\sim 10^{-11}$  Torr a relatively long distance ( $\sim 15$  m) with a number of differentiating vacuum pumped sections were then passed before the injection into the storage ring. The ions are then accelerated using a RF-cavity to the maximum energy of about 96 MeV/ion mass in amu. The low pressure in the storage ring allows long storage times, and infrared active ion vibrations have the time to relax down to their ground state before the data recording starts.

### 2.2 Ion current measurement

Simultaneously with the DR count rate measurement the bunched ion beam current is measured by two different measurement systems. A Bergoz Integrating Current Transformer (ICT) and a sum signal from a capacitive pick-up (PU) are integrated simultaneously. Initially a high current is measured and the ICT signal is then used to calibrate the PU signal. This results in a resolution of 100 pA RMS, where the typical ion current is 1 nA–10  $\mu$ A [23]. This is done during a short time (40 ms) just after the acceleration has finished. By scaling background measurements from a micro channel plate (MCP) located at the end of a straight section to this value it is possible to deduce the coasting ion beam current throughout the whole time of the measurement.

### 2.3 Electron cooler

The electron cooler is used as a tool to reduce the energy spread of the ion beam. Through Coulomb interactions of the ions with the continuously renewed cold electrons the ions experience a drag force when not at the same velocity as the electrons. They are therefore dragged to uniformly follow the velocity of the electrons, which increases the phase space density of the ion beam and therefore decreases the radius of the ion beam. This process is called electron cooling and after acceleration the ions are cooled as described for  $\sim 2$  s. This is significantly less than the required 50 s estimated for the cooling through interaction with the electrons [24], a timescale which would be impossible to achieve due to the limited lifetime of the beam. However, cooling through superelastic collisions and radiative decay of excited states of infrared active

Deleted: e.g.

Deleted: No independent

Deleted: in

Deleted: of the isomerisation

Deleted: given

Deleted: below

Deleted: we assume the isomerisation

Deleted: Beam diameter is now small and divergence sufficiently low for all neutral DR fragments containing C or O to hit the detector.

Deleted: infra-red

Deleted: the

Deleted: a sort of 'friction'/drag

Deleted: electrons which

Deleted: i.e. it

Deleted: ,

Deleted: t

Formatted

Deleted: but limited due to beam lifetime

vibrations is also possible. No data about the lifetimes of these two processes are available for the ions investigated, but lifetimes of the latter one have generally proved to be sufficiently short with other ions. [25] The electron cooler also serves as the interaction region where the electrons can recombine with the ions, which subsequently dissociate into neutral species.

Formatted

Deleted: ions which

## 2.4 Detection

The neutral products are no longer affected by the magnetic field in the bending magnets, and therefore leave the ring tangentially into the 0°-arm of the ring where they impinge on an energy sensitive ion-implanted detector with a diameter of ~34 mm located about 3.8 m from the center of the interaction region. The longitudinal velocities of the fragments are almost identical and the time resolution of the detection system is insufficient to distinguish between the different particles originating from the same DR-event. Therefore the maximum particle energy is always measured, independently of the reaction channel. To distinguish between the different channels a metal foil grid with a well-known transmission probability ( $0.297 \pm 0.015$ ) was inserted [21]. Fragments stopped by the grid are not detected, which causes the single peak spectrum obtained without the grid to split up into one showing different peaks, corresponding to the fragments measured, their intensity depending on the branching ratios. The peak intensities can then be used to determine the branching ratios using a transmission probability matrix for the overall reaction. However, due to the small size of the detector (~17 mm radius) and the high kinetic energy release in some reaction channels, some lighter fragments might have sufficient transversal energy to miss the detector and thus escape detection. Since the diameter of the beam (which can be estimated from the MCP signal) is about 5 mm and divergence sufficiently low, it can be expected that all neutral DR fragments containing heavy atoms (C or O) hit the detector. The centering of the beam on the surface barrier detector has been checked by a phosphorus screen located behind the removable surface detector in the detection arm of the ring.

Deleted: so called

Deleted: -10

## 3 Results

### 3.1 Branching ratios

The branching ratios are defined as the probabilities of producing the different reaction channels. The viable pathways of the DR are given in table 1. A spectrum at ~0 eV collision energy and a background signal recorded at 2 eV relative translational energy of the reactants were measured. At the latter energy the DR cross section is very small, hence the vast majority of the events are assumed to be from background processes. These data were normalized according to the current measurement recorded simultaneously with the spectrum from the ion implant detector. Finally we subtracted the normalized background signal measured at 2 eV from the original MCS spectrum taken at ~0 eV. The resulting spectrum is shown in Fig. 1.

Deleted: processes

Deleted: are

Deleted: and subtracted the spectrum measured at 2 eV from the one obtained at ~0 eV spectrum. The resulting spectrum is shown in Fig. 1.

Fig. 1 BR spectrum

In the case of  $\text{CD}_2\text{OD}^+$ , four peaks in the obtained spectrum could be identified. The peak at highest energy is where all fragments are detected and the three peaks at lower energies correspond to events where 1D, 2D and 3D atoms are lost, respectively. By comparing the areas of these peaks measured we can obtain



information on the extent of the particle loss. Theoretically, five exoergic channels can contribute to the loss detected, which makes an estimate of the relative contributions of these pathways to the overall loss difficult.

To obtain the branching ratio spectra we performed a measurement at  $\sim 0$  eV collision energy (when the ions are tuned to go with the same velocity as the electrons.) with the grid inserted. Due to the longitudinal energy spread of  $\sim 0.1$  meV and the transversal electron temperature of  $\sim 2$  meV [26] the factual interaction energy is of the same order as the transversal electron temperature i.e.  $\sim 2$  meV (but also slightly affected by the energy spread amongst the ions). As in the previous measurement, data obtained at 2 eV were subtracted to obtain a pure DR spectrum, which is shown in Fig. 2.

Deleted: measured

Deleted: collision energy

Deleted: This is done when the ions are tuned to go with the same velocity as the electrons.

Deleted: [

Deleted: but

Deleted: and this is shown

Fig. 2 BR Spectrum

Although the peaks are easily distinguishable in the case of  $\text{CD}_2\text{OD}^+$ , it is difficult to obtain a satisfactory result for the branching due to the problem of particle loss from the different reaction channels. It was decided to eliminate the problem by treating the sum of the C + O + xD peaks as one feature. By using the transmission probability of the grid the following matrix systems was set up:

Eq.1:

$$\begin{pmatrix} I(C + O + xD) \\ I(O + 2D) \\ I(O + D) \\ I(C + 2D) \\ I(C + D) \end{pmatrix} = \begin{pmatrix} P_T & P_T^2 & P_T^2 \\ 0 & P_T(1 - P_T) & 0 \\ 0 & 0 & P_T(1 - P_T) \\ 0 & 0 & P_T(1 - P_T) \\ 0 & P_T(1 - P_T) & 0 \end{pmatrix} * \begin{pmatrix} \alpha \\ \beta \\ \gamma \end{pmatrix},$$

where the leftmost column corresponds to the recorded intensities of the different particles,  $P_T$  is the transmission probability of the grid,  $\alpha$ ,  $\beta$ , and  $\gamma$  are the branching ratios for the different events. For example, consider the second column of the matrix that refers to the channel:  $\text{CD} + \text{D}_2\text{O}$  ( $\beta$ ). For detection of a signal in the C + O + xD peak (first row), both particles have to pass, i.e. the probability is  $P_T^2$ . The next row considers the case if the CD particle is stopped by the grid and only the  $\text{D}_2\text{O}$  continue, which has a probability of  $P_T(1 - P_T)$ . Third and fourth row consider cases with O+D and C+2D, respectively; it is obvious that they cannot be produced by this reaction channel, hence the probability is 0. Finally the fifth row considers the case of  $\text{D}_2\text{O}$  stopped by the grid and the CD fragment passing. The rest of the elements in the matrix are deduced in an analogue way. We used the same matrix system for  $\text{CH}_2\text{OH}^+$  (Eq.2) and undertook the same procedure for  $\text{CD}_2\text{OD}_2^+$  specie, where we in the same manner treated the sum of the C + O + xD peaks as one feature (Eq.3).

Deleted: the

Deleted: specie

Deleted: The

Deleted: was undertaken

Deleted: the

Deleted: two other

Deleted: th

Deleted: ned

Deleted: s

Eq.2:

$$\begin{pmatrix} I(C+O+xH) \\ I(O+2H) \\ I(O+H) \\ I(C+2H) \\ I(C+H) \end{pmatrix} = \begin{pmatrix} P_T & P_T^2 & P_T^2 \\ 0 & P_T(1-P_T) & 0 \\ 0 & 0 & P_T(1-P_T) \\ 0 & 0 & P_T(1-P_T) \\ 0 & P_T(1-P_T) & 0 \end{pmatrix} * \begin{pmatrix} \alpha_2 \\ \beta_2 \\ \gamma_2 \end{pmatrix} \rightarrow$$

Eq.3:

$$\begin{pmatrix} I(C+O+xD) \\ I(O+xD) \\ I(C+xD) \end{pmatrix} = \begin{pmatrix} P_T & P_T^2 \\ 0 & P_T(1-P_T) \\ 0 & P_T(1-P_T) \end{pmatrix} * \begin{pmatrix} \alpha_3 \\ \beta_3 \end{pmatrix} \rightarrow$$

Solving the equation systems gives the following branching fractions:

Table 2. Branching ratios of the DR reaction channels

Ion	Fragments			Branching ratio
CD <sub>2</sub> OD <sup>+</sup>	COD <sub>x</sub>	yD	zD <sub>2</sub>	77 ± 2 %
	CD	D <sub>2</sub> O		5 ± 1 %
	CD <sub>2</sub>	OD		18 ± 2 %
CH <sub>2</sub> OH <sup>+</sup>	COH <sub>x</sub>	yH	zH <sub>2</sub>	92 ± 2 %
	CH	H <sub>2</sub> O		2.2 ± 1 %
	CH <sub>2</sub>	OH		5.5 ± 1 %
CD <sub>2</sub> OD <sub>2</sub> <sup>+</sup>	COD <sub>x</sub>	yD	zD <sub>2</sub>	57 ± 3 %
	CD <sub>x</sub>	OD <sub>y</sub>	zD <sub>2</sub>	43 ± 3 %
			aD	

In the table the letters x are used for denoting the number of hydrogen/deuterium atoms. y, z and a are used for visualization of the possible pathways.

The error bars in the table were achieved by changing the fit of the achieved spectrum to extreme values while still retaining reasonable overlap between the fit and the data.

### 3.2 Absolute cross sections and thermal reaction rate

During the cross sections measurement, the ions were first cooled for ~2 s before the measurements began. Data were obtained during two seconds per cycle. By ramping the electron cooler cathode voltage linearly around the value corresponding to where the electrons and ions have the same velocity, the electrons first travel faster than the ions and subsequently slower. Hence the interaction energy changes from 2 eV down to ~0.2 meV and then up to 2 eV again. All DR events were recorded via a single channel analyzer. In this part of the experiment we tuned the single channel analyzer so events involving a loss of light fragments also got included. The signal was then recorded with a multi channel scaler (4096 channels) as a function of storage

Deleted: -----Page Break-----

Deleted: y

Deleted: rendering

Deleted: in

Deleted: as a signal since we were not interested in what specific reaction channel was active.

Deleted: a

time. Each channel where recording events corresponding to a certain dwell time (typically 2 ms) that in turn corresponds to a certain interaction energy interval. From the spectrum achieved background contributions (constituting the signal at 2 eV collision energy) are subtracted. At the same time as earlier described, we measured the ion current with a combination of an ICT, PU and a MCP. The average DR rate coefficient is given by the formula:

$$\langle v_{cm} \sigma \rangle = \left( \frac{dN}{dt} \right) \frac{v_i v_e e^2 r_e^2 \pi}{I_e I_i l}$$

where  $dN/dt$  is the count rate,  $v_i$  and  $v_e$  are the ion and electron velocities respectively;  $r_e$  is the radius of the electron beam,  $L$  the length of the interaction region, and  $I_i$  and  $I_e$  are the ion and electron current, respectively. The following corrections of the measurement had to be undertaken: The electrons emitted from the electron gun are not accelerated exactly from the cathode potential to the ground potential because the potential difference is reduced by the electron beam space charge potential. As such the voltage of the electron cooler cathode (and therefore  $v_e$ ) had to be corrected. The measured rate coefficient  $\langle v_{cm} \sigma \rangle$  had to be corrected due to toroidal effects in the region where the electron beam is bent into and out of the interaction region [26], and hence the collision energy is larger due to the transversal component of the electron velocity. Finally, the electron beam has, in contrast to the ion beam, a non-negligible velocity spread and the measured reaction rate  $\langle v_{cm} \sigma \rangle$  had to be deconvoluted according to the equation:

$$\langle v_{cm} \sigma \rangle = \int_{-\infty}^{\infty} v_e f(v_e) \sigma(v_e) d^3 v_e$$

where  $f(v_e)$  is the electron velocity distribution. Due to the relatively large mass of the investigated ion, drag force effects [27] were neglected. Fig. 3 shows the absolute DR cross-section for  $\text{CD}_2\text{OD}^+$  as a function of the relative kinetic energy.

Fig. 3

No resonances were discovered during the cross-section measurement, which would imply a contribution of indirect DR process to the observed rate, though it is noted that the absence of resonances does not exclude the presence of an indirect pathway. These data are best fitted by the expression  $\sigma = 7.46 \times 10^{-15} E(\text{eV})^{-1.20} \text{ cm}^2$ . The thermal reaction rate coefficient can be deduced from the cross sections by applying the formula:

$$k(T) = \frac{8\pi m_e}{(2\pi m_e kT)^{3/2}} \int_0^{\infty} E \sigma(E) e^{-\frac{E}{kT}} dE$$

where  $m_e$  is the electron mass,  $E_{cm}$  is the centre of mass energy and  $T$  the temperature. The following temperature dependence of the thermal rate coefficient was fitted for  $\text{CD}_2\text{OD}^+$ :  $7.5 \times 10^{-7} (T/300)^{-0.59} \text{ cm}^3 \text{ mol}^{-1} \text{ s}^{-1}$  for  $\text{CH}_2\text{OH}^+$ :  $7.0 \times 10^{-7} (T/300)^{-0.78} \text{ cm}^3 \text{ mol}^{-1} \text{ s}^{-1}$  and finally for  $\text{CD}_2\text{OD}_2^+$ :  $1.51 \times 10^{-6} (T/300)^{-0.66} \text{ cm}^3 \text{ mol}^{-1} \text{ s}^{-1}$ . In this evaluation we have systematic errors arising from the uncertainty in the length of the

Deleted: constituting

Deleted: again

[4]

Deleted: (2

Deleted: )

[5]

Deleted: 3

[6]

Deleted: 4

Deleted:

interaction region in the electron cooler, the ion beam current, the electron beam current and the electron density. These combined errors are estimated to be ~10 %.

#### 4 Discussion

Measurements of the DR regarding the species discussed in this article have, to the best of our knowledge, not previously been reported. For  $\text{CH}_2\text{OH}^+$  and  $\text{CD}_2\text{OD}^+$  it is interesting to note the considerable difference in the channel leading to  $\text{CD}_2/\text{CH}_2 + \text{OD}/\text{OH}$  for the two species (~15 %). By far the most dominating channels are those where the C-O bond is left intact, indicating that the intermediate neutrals formed in the DR process do not undergo complicated structural arrangements. This is in contrast to results with protonated/deuterated methanol  $\text{CH}_3\text{OH}_2^+ / \text{CD}_3\text{OD}_2^+$  where channels leading to three-body break up dominate [17]. Conversely the C-O bond also is preserved in the DR of  $\text{HCO}^+$  [28]. This behaviour could possibly be a result of the double bond character of the C-O bond in  $\text{CH}_2\text{OH}^+ / \text{CD}_2\text{OD}^+$  although DR is known to often break even the strongest bonds [29]. Further measurements with other similar ions like the  $\text{CNH}_x^+$  group should be undertaken to clarify if there is a true connection between saturation and breakage of the heavy atom bond.

For  $\text{CD}_2\text{OD}_2^+$  we have C-O bond breakage in 43 % of the reactions which clearly is superior to the one for the two other species in the experiment but still less than for the previously investigated protonated/deuterated methanol  $\text{CH}_3\text{OH}_2^+ / \text{CD}_3\text{OD}_2^+$ . This might indicate a trend that in more saturated carbon- and oxygen-containing ions the break-up of the CO bond is more favoured than in less saturated ones. Further experiments with related compounds are planned to clarify this point.

For the  $\text{CH}_3\text{O}^+ / \text{CD}_3\text{O}^+$  ions, two important isomers have been observed experimentally: the methoxy ion  $\text{CH}_3\text{O}^+ / \text{CD}_3\text{O}^+$  and the hydroxymethyl ion  $\text{CH}_2\text{OH}^+ / \text{CD}_2\text{OD}^+$ . The enthalpies of formation ( $\Delta H_f$ ) are 7.29 eV for  $\text{CH}_2\text{OH}^+$  and 8.73 eV for  $\text{CH}_3\text{O}^+$  [30]. According to ab initio calculations of the ionisation energy for  $\text{CH}_2\text{OH}$  ( $C_s$  planar structure) is 7.45 eV, whereas  $\text{CH}_3\text{O}$  has a calculated ionisation energy of 10.78 eV [31]. Photoionisation experiments have also shown a big difference in the ionisation energy for these neutrals, 7.55 eV and 10.73 eV, respectively [32]. Ab initio calculations predicted that the most stable isomer is  $\text{CH}_2\text{OH}^+$  [33] and that the triplet methoxy cation rapidly dissociates to  $\text{HCO}^+$  and  $\text{H}_2$ . Furthermore, the singlet state of  $\text{CH}_3\text{O}^+$ , which lies 40 kcal/mol above the triplet state rearranges to  $\text{CH}_2\text{OH}^+$  without any measurable activation barrier [31]. Other ab initio calculations showed that the excited singlet state of the  $\text{CH}_3\text{O}^+$  ion undergoes a 1,2-hydride shift without an energy barrier to form the  $\text{CH}_2\text{OH}^+$  isomer, whereas the triplet  $\text{CH}_3\text{O}^+$  ion should be stable, but possess a heat of formation 387 kJ/mol above that of  $\text{CH}_2\text{OH}^+$  and is therefore unlikely to be formed [33][34][35]. In the experiment by Zappey *et al.* [35] it was estimated that the lifetime of the  $\text{CD}_3\text{O}^+$  ions entering a RF-only quadrupole is  $\geq 5 \times 10^{-5}$  s, involving a significant loss of  $\text{D}_2$  to form  $\text{DCO}^+$  ions of about 20 % even at this ion lifetime. The authors interpreted the results as a finite lifetime of the triplet state of the methoxy cation with respect to decay into the lower lying singlet state which subsequently collapses to a  $\text{CD}_2\text{OD}^+$  ion with an internal energy content above the threshold for decomposition. With all these observations in mind it is likely that the  $\text{CH}_2\text{OH}^+ / \text{CD}_2\text{OD}^+$  are by far the dominating ion structures present in the ring, given that the ions are stored for ~2 s before measurement start.

For the  $\text{CH}_4\text{O}^+$  ion, the existence of two isomers has been experimentally observed: the methanol radical cation  $\text{CH}_3\text{OH}^+$  and its distonic isomer  $\text{CH}_2\text{OH}_2^+$  called methyleneoxonium radical cation [36]. In contrast to the neutral  $\text{CH}_4\text{O}$  species, where the complex  $\text{CH}_2\text{OH}_2$  is a weak structure, the  $\text{CH}_2\text{OH}_2^+$  ion represents the most stable  $\text{CH}_4\text{O}^+$  isomer. The energy difference between the two isomers has been theoretically calculated

Deleted: big

Deleted: b

Deleted: It is interesting to note the difference in the channel leading to  $\text{CD}_2/\text{CH}_2 + \text{OD}/\text{OH}$  for the two species.

Deleted: more than

Deleted: This in turn indicates considerable structural rearrangements in the neutral intermediate during the DR process.

Deleted: + and

Deleted: Ab

Deleted: has been calculated to be

Deleted: Photoionization

Deleted: it

Deleted: is

to be  $28.6 \text{ kJ mol}^{-1}$  [37] in good agreement with the experimental value reported as  $30 \text{ kJ mol}^{-1}$ . The barrier for the interconversion was found to be  $108 \text{ kJ mol}^{-1}$ . Recent reports about the influence of neutral molecules (e.g. water, the rare gases, CO and H<sub>2</sub> [37][38]) on the conversion of CH<sub>3</sub>OH<sup>+</sup> to CH<sub>2</sub>OH<sub>2</sub><sup>+</sup> showed that the intramolecular hydrogen migration can be catalysed efficiently. No data concerning lifetime of isomeric conversion by the different substances were found. Nevertheless, it is likely that the interconversion lifetime should be shorter than the cooling time.

It is worthwhile to compare our data with the input used in earlier astronomical model calculations. In the model by Meier et al. [9] the rate constants for CH<sub>3</sub>O<sup>+</sup> / CH<sub>2</sub>OH<sup>+</sup> were not taken from experimental data and the rate constants at 300 K were based on results for similar molecules. Prasad & Huntress [39] estimated the total rate constant at 300 K to be  $6.00 \times 10^{-7} \text{ cm}^3 \text{ s}^{-1}$  and assigned equal probability to the three channels listed: CO + H<sub>2</sub> + H; HCO + 2H; H<sub>2</sub>CO + H. Since pathways involving break-up of the CO bond have been found to be relatively unimportant, our measurements are in agreement with this conclusion although we are not able to determine the relative importance of the above-named three channels. Although it was claimed by Huntress and Mitchell that the DR reaction of CH<sub>2</sub>OH<sup>+</sup> is not the major formation mechanism for formaldehyde [40], there exists a theoretical chance for this pathway, since the C-O bond is conserved in 92% of the DR processes of this ion.

In theoretical calculations undertaken by Herbst *et al.* [41] the formation of the different isomeric products HCOH and H<sub>2</sub>CO in the DR of CH<sub>2</sub>OH<sup>+</sup> was investigated. However, since it is impossible to distinguish different isomers, we cannot conclude anything at the moment of the relative importance of these species.

## 5 Conclusion

Measurements of the reaction cross-sections and branching ratios of the dissociative recombination of the ions CH<sub>2</sub>OH<sup>+</sup>, CD<sub>2</sub>OD<sup>+</sup> and CD<sub>2</sub>OD<sub>2</sub><sup>+</sup> have been performed at CRYRING. Channels preserving the C-O bond are dominating in CH<sub>2</sub>OH<sup>+</sup> (92%), CD<sub>2</sub>OD<sup>+</sup> (77%) and, to a lesser extent in CD<sub>2</sub>OD<sub>2</sub><sup>+</sup> (57%). This is in contrast to the CH<sub>3</sub>OH<sub>2</sub><sup>+</sup> ion, where pathways involving breakage the bond between the heavy atoms are the most important ones. The results from these measurements may be useful in astronomical models determining reaction paths and processes in different astrochemical environments.

## 6 Acknowledgements

We thank the staff at the Manne Siegbahn Laboratory for excellent technical support during our measurements.

## Figure Captions

Fig. 1 Mass spectrum of the neutral fragments for the DR of CD<sub>2</sub>OD<sup>+</sup> (background reduced signal from the energy sensitive detector) **without** the grid. The solid line shows the data, whereas the Gaussian fitting curves are shown as dotted lines and the total fit as a dashed line.

**Deleted:** No structure has been observed in the measurements of the cross sections which would imply indirect DR process; however, the opposite is not necessarily implied.

**Deleted:** isomeric products

**Deleted:** The main impact of our measurement is that its results might be used in astronomical models for different astrochemical environments and other plasmas.

Fig. 2 Mass spectrum of the neutral fragments for the DR of  $\text{CD}_2\text{OD}^+$  (background reduced signal from the energy sensitive detector) **with** the grid in position. The solid line shows the data, whereas the Gaussian fitting curves are shown as dotted lines and the total fit as a dashed line.

Fig. 3 Absolute DR cross-section for  $\text{CD}_2\text{OD}^+$  as a function of energy. The dashed line shows the best fit.

[1] S. A. Haider and A. Bhardwaj, *Icarus*, 177(1), 196-216, (2005)

[2] N. L. Ma, B. J. Smith, J. A. Pople and L. Radom, *J. Am. Chem. Soc.*, 113, 7903, (1991)

[3] G. I. Boger, A. Sternberg, Los Alamos National Laboratory, Preprint Archive, Astrophysics, 1-28, (2006)

[4] W. D. Geppert, R. D. Thomas, A. Ehlerding, F. Hellberg, F. Österdahl, M. Hamberg, J. Semaniak, V. Zhaunerchyk, M. Kaminska, A. Källberg, A. Paal and M. Larsson, *J. Phys.: Conf. Ser.*, 4, 26-31, (2005)

[5] J. H. Yee, V. J. Abreu and W. B. Colwell, *Dissociative Recomb., [Int. Conf.]*, Meeting Date 1988, 286-302, (1989)

[6] W. K. Peterson, T. Abe, H. Fukunishi, M. J. Greffen, H. Hayakawa, Y. Kasahara, I. Kimura, A. Matsuoka, T. Mukai, T. Nagatsuma, K. Tsuruda, B. A. Whalen and A. W. Yau, *J. of Geophysic. Res.*, 99(A12), 23257-74, (1994)

[7] N. V. Smirnova, A. N. Lyakhov and S. I. Kozlov, *Adv. Space Res.*, 30(11), 2597-2600, (2002)

[8] A. I. Florescu-Mitchell and J. B. A. Mitchell, *Physics Reports*, 430(5-6), 277-374, (2006)

[9] R. Meier, P. Eberhardt, D. Krankowsky, and R. R. Hodges, *Astron. Astrophys.*, 277, 677, (1993)

[10] J. Geiss, K. Altwegg, E. Anders, H. Balsiger, A. Meier, E. G. Shelley, W.-H. Ip, H. Rosenbauer and M. Neugebauer, *Astron. Astrophys.*, 247, 226-234, (1991)

[11] D. J. DeFrees, A. D. McLean and E. Herbst, *The Astrophysical Journal*, 279, 322-334, (1984)

[12] R. Johnsen, M. Skrzypkowski, T. Gougousi and M. F. Golde, *Dissociative Recombination: Theory, Experiment and Applications IV, Proceedings of the Conference, Stockholm, Sweden, June 16-20, 1999* (2000)

[13] N. G. Adams, C. R. Herd and D. Smith, *J. Chem. Phys.*, 91, 963, (1989)

[14] L. Lammich, H. Kreckel, S. Krohn, M. Lange, D. Schwalm, D. Strasser, A. Wolf and D. Zajfman, *Radiat. Phys. Chem.*, 68(1-2), 175-179, (2003)

Deleted: Journal

Deleted: Geophysical

Deleted: Research

Deleted: ances in

Deleted: each

Deleted: ion

Deleted: ics and

Deleted: istry

[15] D. R. Bates, *Astrophys J.*, 306, L45, (1986)

[16] W. Geppert, A. Ehlerding, F. Hellberg, S. Kalhori, R. D. Thomas, O. Novotny, S. T. Arnold, T. M. Miller, A. A. Viggiano and M. Larsson, *Phys J Rev Lett*, 93(15), (2004)

[17] W. D. Geppert, M. Hamberg, R. D. Thomas, F. Österdahl, F. Hellberg, V. Zhaunerchyk, A. Ehlerding, T. J. Millar, H. Roberts, J. Semaniak, M. af Ugglas, A. Källberg, A. Simonsson, M. Kaminska and M. Larsson, *Faraday Discuss.* 133, 177 (2006)

[18] Robin Garrod, In Hee Park, Paola Caselli and Eric Herbst, *Faraday Discuss.*, (Advance Article), (2006)

[19] NIST Chemistry webBook, <http://webbook.nist.gov>, (2006)

[20] Gas-Phase ion and neutral thermochemistry, *J. Phys. Chem. Ref. data*, vol. 17, suppl. No. 1, (1988)

[21] A. Neau, A. Al-Khalili, S. Rosén, A. Le Padellec, A. M. Derkatch, W. Shi, L. Vikor, M. Larsson, M. B. Nångård, K. Andersson, H. Danared and M. af Ugglas, *J. Chem. Phys.*, 113, 1762, (2000)

[22] F. Österdahl, Lic. Thesis, KTH, Royal Institute of Technology, Sweden, (2006)

[23] A. Paal, A. Simonsson, J. Dietrich and I. Mohos, *Proceedings of EPAC2006*, Edinburgh, Scotland, p. 1196, (2006)

[24] A. Simonsson, private communication

[25] M. Heninger, D. Lauvergnat, J. Lemaire, P. Boissel, G. Mauclaire, R. Marx, *Int. J. Mass Spectrom.* 223, 669 (2003)

[26] A. Lampert, A. Wolf, D. Habs, J. Kenntner, G. Kilgus, D. Schwalm, M. S. Pindzola and N. R. Badnell, *Phys. Rev. A*, 53, 1413, (1996)

[27] A. Neau, Dissociative processes of relevance in low temperature plasmas, PhD thesis, University of Stockholm, Sweden, (2002)

[28] W. D. Geppert, R. Thomas, A. Ehlerding, J. Semaniak, A. Ehlerding, F. Österdahl, M. af Ugglas, N. Djuric, A. Paal and M. Larsson, *Faraday Discuss.*, 127, 425, (2004)

[29] W. D. Geppert, R. D. Thomas, J. Semaniak, A. Ehlerding, T. J. Millar, F. Österdahl, M. af Ugglas, N. Djuric, A. Paal and M. Larsson, *Astrophys. J.*, 609(1, Pt. 1), 459, (2004)

[30] S. G. Lias, J. E. Bartmess, J. F. Liebman, J. L. Holmes, R. D. Levin and W. G. Mallard, *J. Phys. Chem. Ref. Data*, Vol. 17, Suppl. 1, (1988)

[31] L. A. Curtiss, D. Kock and J. A. Pople, *J. Chem. Phys.*, 95(6), (1991)

[32] D. Ruscic, and J. Berkowitz, *J. Chem. Phys.*, 95, 4033, (1991)

Deleted: sica

Deleted: iew

Deleted: ers

Deleted: .

Deleted: Advance Article),

Formatted

Formatted

Formatted

Formatted

Formatted

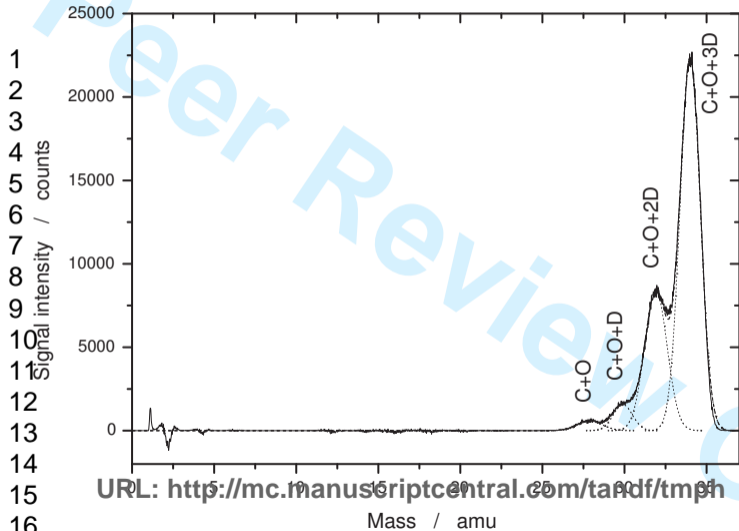
Deleted: Discussions

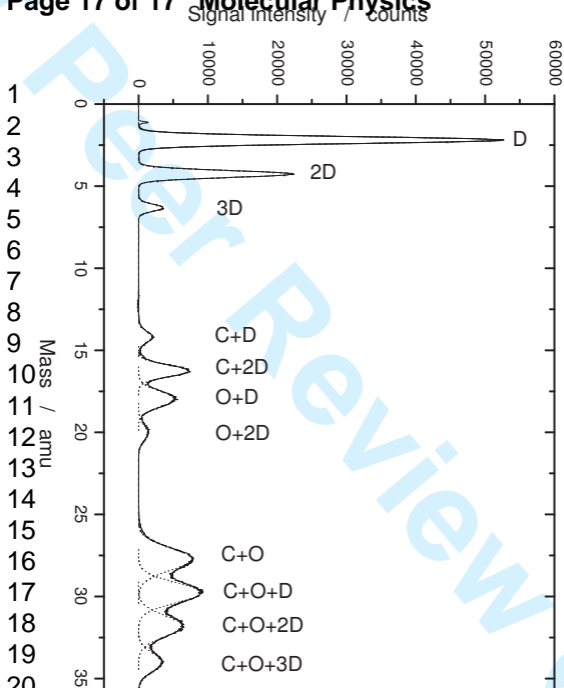
- 1  
2  
3  
4 [33] W. J. Bouma, R. H. Nobes and L. Radom, *Org. Mass. Spectrom.*, 17, 315, (1982)  
5  
6 [34] P. v. R. Schleyer and E. D. Jemmis, *J.C.S. Chem. Comm.*, (1978)  
7  
8 [35] H. W. Zappey, S. Ingemann and N. M. M. Nibbering, *J. Am. Soc. Mass Spectrom.*, 3, 515, (1992)  
9  
10 [36] W. J. Bouma, J.K. MacLeod and L. Radom, *J. Am. Chem. Soc.*, 104(10), 2930, (1982)  
11  
12 [37] J. W. Gauld, H. Audier, J. Fossey, and L. Radom, *J. Am. Chem. Soc.*, 118, 6299, (1996)  
13  
14 [38] T. D. Fridgen, J. M. Parnis, *Int. J. Mass Spectrom.*, 190/191, 181, (1999)  
15  
16 [39] S. S. Prasad, W. T. Huntress, *Astrophys. J. Suppl. Ser.*, 43, 1 (1980)  
17  
18 [40] W. T. Huntress, Jr. and G. F. Mitchell, *The Astrophysical Journal*, 231, 456, (1979)  
19  
20 [41] Y. Osamura, H. Roberts and E. Herbst, *The Astrophysical Journal*, 621, 348, (2005)  
21  
22  
23  
24  
25  
26  
27  
28  
29  
30  
31  
32  
33  
34  
35  
36  
37  
38  
39  
40  
41  
42  
43  
44  
45  
46  
47  
48  
49  
50  
51  
52  
53  
54  
55  
56  
57  
58  
59  
60



Table 1. Open DR reaction channels.

Ion	Fragments			Channel
$\text{CD}_2\text{OD}^+$	$\text{COD}_x$	yD	$\text{zD}_2$	$\alpha$
	CD	$\text{D}_2\text{O}$		$\beta$
	$\text{CD}_2$	OD		$\gamma$
$\text{CH}_2\text{OH}^+$	$\text{COH}_x$	yH	$\text{zH}_2$	$\alpha_2$
	CH	$\text{H}_2\text{O}$		$\beta_2$
	$\text{CH}_2$	OH		$\gamma_2$
$\text{CD}_2\text{OD}_2^+$	$\text{COD}_x$	yD	$\text{zD}_2$	$\alpha_3$
	$\text{CD}_x$	ODy	$\text{zD}_2$	aD $\beta_3$





URL: <http://mc.manuscriptcentral.com/tandf/tmph>

22

23

24

